ChemPhysChem

Research Article
doi.org/10.1002/cphc.202400120

Chemistry Europe
European Chemical Societies Publishing

www.chemphyschem.org

Beyond Electrons: Correlation and Self-Energy in Multicomponent Density Functional Theory

Christof Holzer*[a] and Yannick J. Franzke[b]

Post-Kohn-Sham methods are used to evaluate the ground-state correlation energy and the orbital self-energy of systems consisting of multiple flavors of different fermions. Starting from multicomponent density functional theory, suitable ways to arrive at the corresponding multicomponent random-phase approximation and the multicomponent Green's function *GW* approximation, including relativistic effects, are outlined. Given the importance of both of this methods in the development of modern Kohn–Sham density functional approximations, this work will provide a foundation to design advanced multi-component density functional approximations. Additionally, the *GW* quasiparticle energies are needed to study light-matter interactions with the Bethe-Salpeter equation.

1. Introduction

Multicomponent density functional theory (MC–DFT) has emerged as the many-fermion version of density functional theory.[1–4] Prime examples for applications of MC–DFT are systems containing electrons and protons, with MC–DFT being able to go beyond the Born–Oppenheimer approximation.[5–9] Significant progress on this topic has been achieved in the last two decades, including the development of time-dependent MC–DFT,[10–17] electron-proton correlation functionals,[2,18–25] and electron-muon correlation functionals.[26,27]

The interaction between the different fermions in multi-component DFT is of special interest, describing the intricate correlation in movement between, for example, electrons and protons or other femions. As outlined above, notable efforts have been put into the development of electron-proton correlation density functionals. It was found that these correlation effects are rather important for the description of proton binding energies and subsequently proton affinities.[6] Random phase approximation (RPA) methods[28–40] have been at the heart of developing correlation functionals since the beginning of development of modern density functional approximations, but have also recently been used to design new approximations.[41–44] An extension of RPA to the framework of multicomponent DFT is therefore promising for a further understanding of the aforementioned electron-proton interaction, and more generally electron-fermion interactions. Targeting robust multicomponent Kohn–Sham density functional approximations, using the RPA new sophisticated density functional approximations can be constructed. Similar views hold for many-body Green's function *GW* approaches,[45–56] which have successfully emerged as useful electronic post-Kohn–Sham methods, providing a way to accurately predict ionization energies and band gaps. While *GW* has earlier been shown to yield promising results for H_2 and muon dimer energies,[57,58] it can also be immensely helpful in providing an accurate description of proton or fermion binding energies in general.

Herein, we present the derivation, implementation, and assessment of the RPA correlation energy and the *GW* self-energy based on multicomponent DFT. Efficiency is ensured with the so-called density-fitting or resolution-of-the-identity (RI) approximation, similar to the electron-only limit.[31,36,59–64] Further, explicit relativistic corrections are discussed to study molecules with heavy elements. This way, we develop practical multicomponent post-Kohn–Sham methods, which can be used to design accurate electron-proton and more general electron-fermion correlation functionals.

2. Theory

2.1. Notation

Basis functions are indicated by χ with Greek indices, while the one-particle Kohn–Sham (KS) states, ϕ, use Latin indices. Thus, the KS states of two fermions in the basis set approximation read

$$q' = \phi_{q'}(x) = \sum_{\mu} c_{\mu\sigma,q'} \chi_{\mu'}(r) \tag{1}$$

[a] Dr. C. Holzer
Karlsruhe Institute of Technology (KIT)
Institute of Theoretical Solid State Physics
Kaiserstraße 12
76131 Karlsruhe (Germany)
E-mail: christof.holzer@kit.edu

[b] Dr. Y. J. Franzke
Friedrich Schiller University Jena
Otto Schott Institute of Materials Research
Löbdergraben 32
07743 Jena (Germany)

Supporting information for this article is available on the WWW under https://doi.org/10.1002/cphc.202400120

$$q'' = \phi_{q''}(x) = \sum_{\mu} c_{\mu\sigma,q''}\chi_{\mu''}(r). \tag{2}$$

Here, σ denotes the spin of the fermion and x is a combined spin and spatial coordinate. An unprimed index p will be used to denote combined spaces of fermion **1**′ and fermion **2**″,

$$q = \{q', q''\} = \{\phi_{q'}(x), \phi_{q''}(x)\} \tag{3}$$

The sets of orbitals q' and q'' are obtained from multicomponent DFT as outlined in literature.[1–3]

2.2. Correlation Energies from the Random-Phase Approximation in Multicomponent DFT

Starting from a ground-state solution, where the fermions **1**′ and **2**″ are coupled solely via Coulomb interactions, the random phase approximation can be used to recover the missing correlation part. Following the formalism of Perdew and Langreth,[28] the correlation energy in the RPA is defined as[28,39,64]

$$E^{\mathrm{C,RPA}} = \int_{-\infty}^{\infty} \frac{d\omega}{4\pi} \mathrm{Tr}[\ln(\mathbf{1} + \chi_0(i\omega)\mathbf{v}) - \chi_0(i\omega)\mathbf{v})] \tag{4}$$

and can easily be extended to multicomponent DFT references. Simply let $\chi_0(\omega)$, referring to the non-interacting KS response function,

$$\chi_0(\omega)_{kc,kc} = (\varepsilon_{k'} - \varepsilon_{c'} + \omega)^{-1} + (\varepsilon_{k''} - \varepsilon_{c''} + \omega)^{-1} \tag{5}$$

$$\chi_0(\omega)_{ck,ck} = (\varepsilon_{k'} - \varepsilon_{c'} - \omega)^{-1} + (\varepsilon_{k''} - \varepsilon_{c''} - \omega)^{-1}, \tag{6}$$

encompass the whole space of available fermions. ε_q denotes the corresponding eigenvalue of the q-th KS eigenstate, and **v** is a Coulomb integral matrix

$$v_{pq,rs} = (pq|rs) = Q_1 Q_2 \int\int dx_1 dx_2 \phi_p^*(x_1)\phi_q(x_1)\tfrac{1}{r_{12}}\phi_r^*(x_2)\phi_s(x_2), \tag{7}$$

where Q refers to the charge of the corresponding fermion. In its matrix form, **v** therefore adopts a block structure, with the diagonal blocks being occupied by the same-fermion Coulomb integrals, and the off-diagonal blocks being occupied by the other-fermion integrals. Following the derivation of Furche,[30] it is straightforward to arrive at the plasmon formula for the total correlation energy within the RPA for a multicomponent DFT reference. The resulting expression is

$$E^{\mathrm{C,RPA}} = \frac{1}{2}\sum_n \left(\Omega_n^+\right) - \mathrm{Tr}(\mathbf{A}') - \mathrm{Tr}(\mathbf{A}''), \tag{8}$$

with the excitation energies Ω_n being obtained from

$$\Delta(X, Y) = -\omega\Lambda(X, Y) \tag{9}$$

with the supermatrices

$$\Delta = \begin{pmatrix} \mathbf{A}' & \mathbf{B}' & (\mathbf{C}^{\mathbf{1}})^{\dagger} & (\mathbf{C}^{\mathbf{2}})^{\dagger} \\ (\mathbf{B}')^{*} & (\mathbf{A}')^{*} & (\mathbf{C}^{\mathbf{2}})^{\mathsf{T}} & (\mathbf{C}^{\mathbf{1}})^{\mathsf{T}} \\ \mathbf{C}^{\mathbf{1}} & \mathbf{C}^{\mathbf{2}} & \mathbf{A}'' & \mathbf{B}'' \\ (\mathbf{C}^{\mathbf{2}})^{*} & (\mathbf{C}^{\mathbf{1}})^{*} & (\mathbf{B}'')^{*} & (\mathbf{A}'')^{*} \end{pmatrix} \tag{10}$$

and

$$\Lambda = \begin{pmatrix} \mathbf{1} & \mathbf{0} & \mathbf{0} & \mathbf{0} \\ \mathbf{0} & -\mathbf{1} & \mathbf{0} & \mathbf{0} \\ \mathbf{0} & \mathbf{0} & \mathbf{1} & \mathbf{0} \\ \mathbf{0} & \mathbf{0} & \mathbf{0} & -\mathbf{1} \end{pmatrix}. \tag{11}$$

The matrices **A**, **B**, and **C** are defined as

$$A_{a'i',b'j'} = (\varepsilon_{a'} - \varepsilon_{i'})\delta_{i'j'}\delta a'b' + (a'i'|j'b') \tag{12}$$

$$B_{a'i',b'j'} = (a'i'|b'j') \tag{13}$$

$$C^1_{a'i',b''j''} = (a'i'|j''b'') \tag{14}$$

$$C^2_{a'i',b''j''} = (a'i'|b''j''). \tag{15}$$

The corresponding matrices **A**″ and **B**″ are obtained by replacing the single primes quantities with their double primed analogues. Subsequently subtracting the RPA correlation energies of the isolated fermion systems, $E_{\mathrm{A}}^{\mathrm{C,RPA}}$ and $E_{\mathrm{B}}^{\mathrm{C,RPA}}$, yields the inter-fermion part of the correlation energy,

$$E_{\mathrm{A}\circ\mathrm{B}}^{\mathrm{C,RPA}} = E_{\mathrm{tot.}}^{\mathrm{C,RPA}} - E_{\mathrm{A}}^{\mathrm{C,RPA}} - E_{\mathrm{B}}^{\mathrm{C,RPA}}. \tag{16}$$

Eq. 16 will approximately cancel self-interactions errors between the same type of fermions. The latter property is important in cases where large self-interactions errors are expected, as for example for protons. While it is computationally more efficient to evaluate $E_{\mathrm{A}}^{\mathrm{C,RPA}}$ and $E_{\mathrm{B}}^{\mathrm{C,RPA}}$ separately, the sum of them can conveniently be obtained by setting $\mathbf{C}^{\mathbf{1}} = \mathbf{C}^{\mathbf{2}} = 0$ in Eq. 10. We note in passing that Eqs. 10 and 16 can be extended to more than two different fermions in a straightforward manner.

2.3. Auxiliary Subspace Approach for the Multicomponent Random-Phase Approximation

While convenient for initial reference results, the direct evaluation of Eq. 16 via Eq. 10 is rather demanding. It steeply grows with the total number of interacting fermions as $\mathcal{O}(N^6)$, being unfeasible for applying it to more than a few atoms or

when extended basis sets are used. Similar to the standard electron-only RPA,[31,36,60,63,64] the required effort can still be drastically lowered by introducing the multicomponent resolution-of-the-identity (MC-RI) approximation. The latter has already been outlined for MC–DFT,[65–68] and can be adapted to post-KS methods in a straightforward manner defining

$$v_{p'q',r''s''} \approx \sum_R B_{R,p'q'} B^*_{R,r''s''} \tag{17}$$

$$B_{R,r's'} = Q' \sum_S [V^{-1/2}]_{RS} (S|r's') \tag{18}$$

$$V_{RS} = (R|S), \tag{19}$$

In the MC-RI approach, the 3-index quantities $R_{P,r's'}$ carry information about the charge of the particle, yielding the correct sign for the Coulomb interaction between different. Using the MC-RI approximation, and following Refs. [64] and [60], the total RPA correlation energy can be calculated as

$$E^{\mathrm{C,MC-RI-RPA}} = \int_{-\infty}^{\infty} \frac{d\omega}{4\pi} (\{\ln(\det[\mathbf{1} + \Pi_{RS}(i\omega)])\} - \mathrm{tr}[\Pi_{RS}(i\omega)]) \tag{20}$$

with the combined intra- and inter-fermion interaction kernel $\Pi_{RS}(\omega)$ given by

$$\Pi_{RS}(\omega) = \sum_{kc} \left[\frac{B_{R,kc} B^*_{S,kc}}{\varepsilon_c - \varepsilon_k + \omega} + \frac{B_{R,c'k} B^*_{S,c'k}}{\varepsilon_{c'} - \varepsilon_k - \omega} \right] + \sum_{k'c'} \left[\frac{B_{R,k'c'} B^*_{S,k'c'}}{\varepsilon_{c'} - \varepsilon_{k'} + \omega} + \frac{B_{R,c'k'} B^*_{S,c'k'}}{\varepsilon_{c'} - \varepsilon_{k'} - \omega} \right]. \tag{21}$$

Remarkably, Eq. 21 projects the interaction kernel for both fermions into a common auxiliary subspace. A common auxiliary subspace, defined by a common set of auxiliary basis functions, χ_R, must therefore be chosen for all fermions. This subspace must be flexible enough to project the Hilbert spaces of both electrons and the other fermion into a common Hilbert space, likely requiring a sharp increase in the number of auxiliary basis functions employed. Note that this statement remains valid for an arbitrary number of different fermions. Assume a set of k different fermionic systems, with each featuring N unique fermions. Then the evaluation of Eq. 10 scales as $\mathcal{O}([k \cdot N]^6)$, being *exponential* with the number of distinguishable fermionic systems. Contrary, the evaluation of Eq. 21 scales as $\mathcal{O}(k \cdot N^4)$, growing only *linear* with the number of different fermions considered in the multicomponent DFT approach. The only downside of Eq. 21, and generally the MC-RI approach, is that the chosen auxiliary basis functions must be able to cover all interacting fermions accurately. The equivalence of the RPA correlation energies obtained from Eqs. 8 and 20 for MC–DFT references was numerically verified.

If the auxiliary basis sets for both fermions are chosen to coincide, the stabilized Coulomb energy of the ground-state also takes a particularly simple form.[69] Defining

$$\gamma'_R = \sum_{p',q'} (R|p'q') D_{p'q'} \tag{22}$$

$$\Gamma'_R = \sum_S (R|S)^{-1} \gamma'_S, \tag{23}$$

the stabilized vector y' is obtained as

$$x'_R = \gamma'_R - \sum_S (R|S) \Gamma'_S \tag{24}$$

$$y'_R = \Gamma'_R + \sum_S (R|S)^{-1} x'_S. \tag{25}$$

The stabilized Coulomb energy of the fermionic system $\mathbf{1}'$ in the presence of $\mathbf{2}''$ is then obtained as

$$E^{\mathrm{Coul.}}_{\mathbf{1}'} = \sum_R (Q'Q'\gamma'_R + Q'Q''\gamma''_R)\Gamma'_R - \frac{1}{2}\sum_R (Q'Q'y'_R + Q'Q''y''_R)\Gamma'_R. \tag{26}$$

For the Coulomb energy of fermionic system $\mathbf{2}''$, the fermionic index of the quantities Γ, γ, and y simply needs to be switched. As Eqs. 22 and 25 need to be evaluated also in standard electronic RI-Coulomb approximation, the evaluation of Eq. 26 in the MC-RI is straightforward. Note that this RI variant is not restricted to RPA and *GW* but also applicable to post-Hartree–Fock approaches such as second-order Møller–Plesset perturbation theory (MP2).

2.4. Correlation Part of the Fermion Self-Energy of Multicomponent Kohn–Sham Eigenstates

Similar to the particle propagator method for multicomponent wavefunctions,[70] self-energies can also be evaluated for a KS eigenstate obtained from MC–DFT. Using the *GW* approximation,[45] the self-energy $\Sigma(x, x', \omega)$ is obtained as

$$\Sigma(x, x', \omega) = \frac{1}{2\pi i} \int_{-\infty}^{\infty} d\omega' e^{i\omega' 0^+} W(x, x', \omega') G(x, x', \omega + \omega'), \tag{27}$$

which is calculated from the multicomponent Green's function

$$G(x, x', \omega) = \sum_{q'} \frac{\phi_{q'}(x)\phi^*_{q'}(x')}{\omega - \varepsilon^F_{q'} + i\delta sgn(\varepsilon^F_{q'})} + \sum_{q''} \frac{\phi_{q''}(x)\phi^*_{q''}(x')}{\omega - \varepsilon^F_{q''} + i\delta sgn(\varepsilon^F_{q''})} \tag{28}$$

and the screened exchange

$$W(x, x', \omega) = \int dx'' \kappa^{-1}(x, x'', \omega) v(r'' - r'), \tag{29}$$

where $\varepsilon_q^F = \varepsilon_q - \varepsilon^F$ is the difference between the energy of q-th KS eigenstate and the Fermi level of the respective fermion. The dielectric function κ is defined as

$$\kappa_{pq,rs}(\omega) = \mathbf{1} - \sum_{tu} \chi_0(\omega)_{pq,tu} v_{tu,rs}, \tag{30}$$

where it is recalled that indices $p, q \ldots$ run over all different fermion orbitals. Therefore, χ_0 and **v** represent supermatrices encompassing all different fermions as outlined by Eqs. 5 to 7. Using Eq. 30 and the MC-RI approximation, Eq. 29 can be rewritten as

$$W_{pq,rs}(\omega) = \sum_{RS} B^*_{R,pq} [\mathbf{1} + \Pi_{RS}(\omega)]^{-1} B_{S,rs}, \tag{31}$$

where we remind the reader that $p = p', p''$, and therefore **W** assumes a blocked structure for the two different fermion systems. Using contour deformation,[63,64,71] an explicit formula for the diagonal elements of the correlation part of the self-energy can be obtained as

$$\Sigma^C_q(\omega^F) = R^C_q(\omega^F) + I^C_q(\omega^F). \tag{32}$$

The terms $I^C_q(\omega^F)$ and $R^C_q(\omega^F)$, can be defined analogous to standard *GW* methods,

$$I^C_{q'}(\omega^F) = -\frac{1}{4\pi} \sum_{p'} \int_{-\infty}^{\infty} d\omega' \frac{W^C_{p'q',p'q'}(i\omega')}{\omega^F - \varepsilon^F_{p'} + \omega'} \tag{33}$$

$$R^C_{q'}(\omega^F) = \sum_{p'} \int_{p'} \left\{ W^C_{p'q',p'q'}(\omega^F - \varepsilon^F_{p'}) \right\}. \tag{34}$$

$f_{p'}$ is the contribution of the residue as defined by Eq. (20) of Ref. [64]. The superscript in the frequency, ω^F, again denotes that the frequency is to be taken with respect to the Fermi level. The correlation part of the screened exchange is obtained by subtracting the Coulomb part,

$$W^C_{p'q',r's'}(\omega') = W_{p'q',r's'}(\omega') - v_{p'q',r's'}. \tag{35}$$

Interestingly, cross-fermion terms only enter Eqs. 33 and 34 implicitly through **W**, which depends on all fermions via the dielectric matrix κ in the auxiliary subspace representations, as outlined in Eq. 30. Quasiparticle energies are then obtained from the self-energy and the eigenvalues of the KS eigenstates in the usual manner as

$$\varepsilon^{QP}_{q'}(\omega) = \varepsilon^{KS}_{q'} + Z\langle q'|\Sigma^X_{q'} + \Sigma^C_{q'}(\omega) - V^{KS}_{q'}|q'\rangle. \tag{36}$$

In the linearized G_0W_0 approach, the quasiparticle energies are obtained by evaluating $\Sigma^C_{p'}$ at the energy of the corresponding orbital p', and simply applying a linearization factor Z to arrive at a solution.[47] Eigenvalue self-consistent *GW*, ev*GW*, furthermore takes into account that the solution depends on itself, and also re-enter Eq. 27 through the updated matrices **G** and **W**, requiring an iterative solution of the problem. Note here that an update of the quasiparticle energies $\varepsilon^{QP}_{q'}$ necessitates also an update of $\varepsilon^{QP}_{q''}$ in the next iteration. Freezing the quasiparticle states of one fermion will lead to a loss of correlation information in the system.

2.5. Self-Screening Errors in the Self-Energy of Multicomponent Kohn–Sham Eigenstates

While often neglected for electrons within the *GW* approximation, self-screening may lead to catastrophic errors for different fermions. Especially the heavier, more localized protons are indeed prone to suffer from this issue. Given a system consisting of N electrons and a single fermion q'' other than an electron, the noninteracting Green's function outlined in Eq. 28 takes the form

$$G(x,x',\omega) = \sum_{q'}^{N} \frac{\phi_{q'}(x)\phi^*_{q'}(x')}{\omega - \varepsilon^F_{q'} + i\delta sgn(\varepsilon^F_{q'})} + \frac{\phi_{q''}(x)\phi^*_{q''}(x')}{\omega - \varepsilon^F_{q''} + i\delta sgn(\varepsilon^F_{p''})}. \tag{37}$$

Using Eq. 37 to evaluate the correlation part of the self-energy for the fermion q'' will then lead to considerable self-screening errors which, for protons, can reach a few eV in magnitude. Clearly, the single fermion q'' must not screen itself in the contribution to **W**. To remedy this issue, the self-screening correction reported by Aryasetiawan *et al.* can be employed.[48] By subtracting the spin-orbital Green's function

$$g_{q''}(x,x',\omega) = \frac{\phi_{q''}(x)\phi^*_{q''}(x')}{\omega - \varepsilon^F_{q''} + i\delta sgn(\varepsilon^F_{q''})} \tag{38}$$

from the non-interacting Green's function

$$G^{SSC}_{q''}(x,x',\omega) = G(x,x',\omega) - g_{q''}(x,x',\omega) \tag{39}$$

this erroneous contribution can be rectified. The screened exchange contribution **W** calculated from $G^{SSC}(x,x',\omega)$ therefore reads

$$W^{SSC}_{p'q',r''s''}(\omega) = \sum_{RS} B^*_{R,p'q'} \left[1 + \Pi^{SSC}_{RS}(\omega)\right]^{-1} B_{S,r''s''} \tag{40}$$

With

$$\Pi^{SSC}_{RS}(\omega) = \sum_{k'c'} \left[\frac{B_{P,k'c'} B^*_{Q,k'c'}}{\varepsilon_{c'} - \varepsilon_{k'} + \omega} + \frac{B_{P,c'k'} B^*_{Q,c'k'}}{\varepsilon_{c'} - \varepsilon_{k'} - \omega} \right] + \sum_{k''c''} \left[\frac{B_{P,k''c''} B^*_{Q,k''c''}}{\varepsilon_{c''} - \varepsilon_{k''} + \omega} + \frac{B_{P,c''k''} B^*_{Q,c''k''}}{\varepsilon_{c''} - \varepsilon_{k''} - \omega} \right] - \left[\frac{B_{P,q''c''} B^*_{Q,q''c''}}{\varepsilon_{c''} - \varepsilon_{q''} + \omega} + \frac{B_{P,c''q''} B^*_{Q,c''q''}}{\varepsilon_{c''} - \varepsilon_{q''} - \omega} \right] \tag{41}$$

where for a system with a single fermion q'' the last two lines exactly cancel. As outlined in Ref. [48], for a system with many fermions this approach takes vertex corrections in form of exchange diagrams into account. For a proton coupled to a system of many electrons, this actually equals to accounting for all vertex corrections, as in this case the full cancellation is exact. Remaining errors still enter through the imperfect description of the screening through the electrons. The self-screening corrected correlation part of the self-energy is finally obtained by replacing **W** in Eqs. 33 and 34 by the corresponding matrix elements of $\mathbf{W}^{SSC}$.

2.6. Exact Two-Component Transformation for Fermions

To study heavy elements and all energetic regions, relativistic methods are needed.[72–78] Here, a slightly adapted version of the one-electron exact two-component (X2C) Hamiltonian[79–90] can be used for taking into account relativistic effects also for heavier fermions. The respective implementation is straightforward based on an existing electronic code and only requires minor modifications of the decoupling scheme. In Eq. (14) of Ref. [91], the matrix $\mathbb{K}$ is replaced by the proper mass-dependent matrix,

$$\mathbb{K} = \begin{pmatrix} \mathbf{K} & \mathbf{0} \\ \mathbf{0} & 2c\sqrt{m}\mathbf{K}p^{-1} \end{pmatrix} \tag{42}$$

with c denoting the speed of light ($c = 137.0359990840$ in atomic units). This modified matrix $\mathbb{K}$ then again diagonalizes the non-unit metric occurring in the matrix representation of the one-electron Dirac equation as outlined by Eqs. (1) and (14) in Ref. [91] for general fermions with their mass in atomic units deviating from 1. This allows us to use more efficient routines for the diagonalization of the corresponding Dirac matrix. In addition to the trivial adaption of the the nucleus-fermion potential **V** and the kinetic energy matrix **T**, the relativistically modified potential matrix $\widetilde{\mathbf{W}}_{X2C}$ takes the form

$$\widetilde{\mathbf{W}}_{X2C} = p^{-1}\sqrt{m}\mathbf{K}(\mathbf{W}_{X2C})\mathbf{K}\sqrt{m}p^{-1}. \tag{43}$$

Here, we added the subscript X2C for the relativistically modified potential **W** to distinguish it from the screened exchange contribution of the *GW* ansatz. Applying this adaption to the X2C procedure allows for a relativistic transformation of protons (and other fermions) in the vicinity of heavy nuclei, as for example in the Ag and Os clusters outlined in Sec. 3 of this work. The reduction from the complex two-component spin-orbit ansatz to the real one-component scalar-relativistic approach is done in the same fashion as for electrons.[91] For simplicity, we only consider the scalar-relativistic ansatz in the present work. We note in passing that other relativistic approaches such as the Douglas–Kroll–Hess[92–96] or the Barysz–Sadlej–Snijders ansätze[97–100] can be implemented in the same way.

For large systems, local approximations are desirable as the X2C decoupling step is carried out in the decontracted basis.[101,102] The extension of the diagonal local approximation to the unitary decoupling transformation[91,103] (DLU) for general fermions follows accordingly. Further speed-ups are possible by approximating the atomic off-diagonal block of a spatially well separated pair with the non-relativistic limit. Similar to Refs. [104] and [105], we currently use a screening criterion of 12.0 bohr by default. In the course of the present work, this low-scaling DLU scheme was implemented for all X2C modules in TURBOMOLE.[91,106–119]

Computational Methods

The multicomponent RI, RPA, contour deformation *GW*, and *GW* methods including self-screening corrections have been implemented into a development version of TURBOMOLE V7.8.1 (modules ridft, escf, ricc2).[120–123] KS reference solutions are supported up to the class of meta-generalized gradient approximations and local hybrid functionals,[124] using seminumerical integration.[125–128] RPA and *GW* calculations including self-screening corrections were performed at the TMHF[129] local-hybrid functional level of theory. TMHF was used for the electronic and protonic part. As a position-dependent local hybrid functional with the possibility of switching to full exact exchange, it is particularly well suited for MC–DFT, as the additional flexibility allows it to describe both fermions equally well. Especially for strongly localized protons, TMHF will accordingly use 100% exact exchange for their description. All calculations made use of the MC-RI approximation, which is also used for the respective KS ground-state calculations.

We study the quasiparticle and correlation energies for a set of 32 molecular systems, which is based on that of Ref. [6]. The def2-QZVPP electronic basis set was employed for classic nuclei,[130] while the def2-QZVPP-mc electronic basis set was used for quantum protons. The latter basis set is a unity of the decontracted def2-QZVPP basis set and the steep additional functions optimized in Ref. [131]. For quantum protons, additionally the PB5-G protonic basis set was employed.[132] Quantum proton basis functions are centered at the classically optimized proton position. Auxiliary basis sets were chosen accordingly, i.e. available electronic sets were used.[133] For the quantum protons, auxiliary basis sets were generated using the automatic procedure[134,135] of ERKALE[136] from a unity of the electronic and protonic basis sets. To consistently cover all fitting cases in the auxiliary basis set, the electronic cc-pV6Z basis set was combined with an even tempered 10s10p10d10f nuclear basis set with $\alpha = 2\sqrt{2}$ and $\beta = \sqrt{2}$. A threshold of 10^{-7} was chosen in the Cholesky decomposition while generating the auxiliary basis set. From the resulting primitive auxiliary basis set, the high-angular momentum ($l > 6$) functions are subsequently dropped.[135] The resulting auxiliary basis set consistently yields fitting errors of less than 10^{-7} Hartree in the stabilized Coulomb energy. Medium-sized integration grids were used for the TMHF functional (gridsize 3).[137,138] To illustrate the applicability to systems with heavy elements a model for the Ag_3H hydrogen transfer complex of Ref. [139], denoted as L-Ag_3H, and $Os(CO)_{10}H_2$[140] are included in the set. For these molecules, the scalar-relativistic DLU–X2C approach is applied, while calculations for all other molecules use the non-relativistic framework. Relativistic calculations apply the finite nucleus model with parameters taken from Ref. [141]. Here, the all-electron x2c-QZVPPall[142] (Ag, Os) and x2c-TZVPPall[143] (C,N,O,H) basis sets were used for these two complexes. For the quantum hydrogens, the def2-QZVP-mc electronic and PB5-G protonic basis set[132] were again used. Note

that the def2 and x2c-type basis sets are identical for hydrogen. The x2c-type electronic auxiliary bases[143] and the even-tempered protonic auxiliary basis were employed. Tailored grids for relativistic approaches (gridsize 2a) were applied for the TMHF functional.[144]

All structures were optimized using the TMHF functional and the basis sets described before, with the exception of $HeHHe^+$, for which the experimental structure was taken.[145] For the structure optimization, the standard electronic DFT approach was applied. To estimate the reorganization energy of carboxylates upon the loss of a proton, the $HCOO^-$ anion was optimized. The reorganization energy was subsequently obtained from the difference between HCOOH at the optimized structure and the protonated $HCOO^-$ structure.

Multicomponent self-consistent field (MC-SCF) energies were converged with a threshold of 10^{-9} Hartree for the energy and 10^{-6} for the root mean square of the density matrix change. The MC-SCF procedure was converged with a multicomponent augmented Roothaan–Hall solver,[146] which uses macro-iterations for the electronic wavefunction and micro-iterations for the protonic wavefunction.

3. Results and Discussion

Figure 1 outlines the trend of electron-proton (e-p) correlation energies obtained from the RI-RPA and RI-MP2 for a set of 31 molecules, with the quantum protons being marked in bold. Here, RPA and MP2 yield the same trend for most molecular systems, with the MP2 electron-correlation energies being larger by about 2.5 mHartree per proton. The largest e-p correlation energies are found for methane and methanol, followed by water and the positively charged amines with more than one substituent attached to the nitrogen atom. For carboxylates, only minor effects can be spotted depending on the substituents. Attaching fluorine and chlorine atoms to the neighboring groups removes electron density from the acidic proton, leading to a decrease in e-p correlation. However, this effect is not increasing with the number of fluorine atoms, and

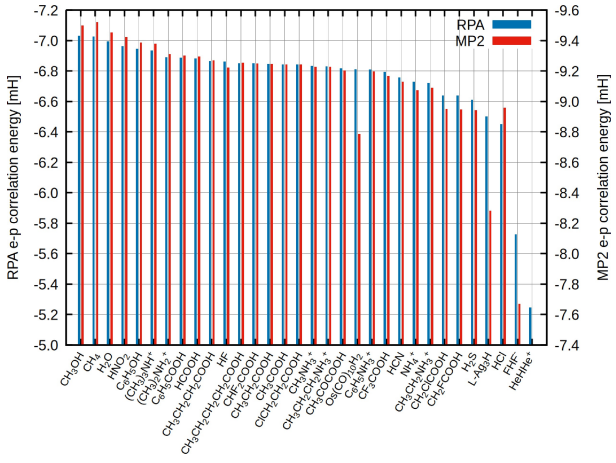

Figure 1. RPA and MP2 correlation energies for 31 molecular systems in milli-Hartree. RPA correlation energies were obtained at a TMHF Kohn–Sham reference and MP2 energies at a Hartree–Fock reference. The MC-RI approximation is used throughout.

both RPA and MP2 predict the e-p correlation energy for the acidic proton in CH_2FCOOH to be lower than in the fully fluorinated species CF_3COOH. Notably, while the the e-p correlation energies for these molecules are difficult to interpret, hinting at a complicated interplay of e-e and e-p correlation, the quasiparticle energies of the acidic protons aligns well with the experimentally found proton affinity as outlined in Table 1.

For the metal-organic molecules L-Ag_3H, $Os(CO)_{10}H_2$, and also for the inorganic FHF^- molecule, deviations from the trend between RPA and MP2 are found. In all cases, the gap between RPA and MP2 is diminished, with differences only amounting to 1.5–2 mHartree per proton. The metal centers as well as the presence of two fluorine atoms leads to highly correlated systems, where e-e and e-p correlation are expected to be strongly coupled and dependent on each other. Especially $HeHHe^+$ and FHF^- also exhibits a consistently lower e-p correlation compared to all other systems. The latter effect can be related to low overall electron density at the average location of the proton, due to the high electron affinity of He and F. This is of special importance, as FHF^- has played a crucial role in the parametrization of e-p correlation functionals.[23–25] For instance, for the epc17-1 functional three parameters of the functional were specifically adapted to fit the proton density of FHF^-.[23] While Hartree-Fock and MC-DFT without e-p correlation lead to too localized proton densities, using the outlier case of FHF^- could bias the calculations towards too delocalized proton densities for other systems. Later parametrizations of e-p correlation functionals also took HCN into account.[24,25] Figure 1 reveals that the latter is better behaved in terms of the comparability to standard organic and metal-organic molecules, with the resulting parametrization being more suitable for general purpose MC-DFT. We finally note that neither the provided RPA nor the MP2 e-p correlation energies are to be understood as reference values. Table 1 and Figure 1 instead shall provide guiding indicators of the magnitude and variance of the e-p correlation in various chemical environments.

Turning to proton affinities, the latter can be obtained from the quasiparticle states obtained via the *GW* approach as outlined in section 2.4. Accordingly, the quasiparticle energy is related to the proton affinity simply as[6,70]

$$\mathrm{PA}(A) = E_A - E_{\mathrm{AH^+}} + \frac{5}{2}RT \approx -\varepsilon^{\mathrm{QP}}_{\mathrm{A,HOMO''}} + \frac{5}{2}RT, \tag{44}$$

with $\frac{5}{2}RT \approx 0.064$ eV. The equivalence is only approximate, because within the *GW* approximation, the geometric relaxation of the deprotonated molecule is neglected. The calculated G_0W_0 and ev*GW* quasiparticle energies as well as KS orbital energies of the highest occupied quantum proton orbital are listed in Table 1.

The trends shown in Table 1 outline that the correction stemming from the correlation part of the self-energy is comparably large for protons, being of the order of a few eV. Similar to HF,[155] there is a near-linear correlation between the protonic KS HOMO and the proton affinity. However, the deviation between $-\varepsilon^{\mathrm{KS}}_{p''}$ and the proton affinity is comparably

Table 1. RPA electron-proton correlation energy $E_{e-p}^{C,RPA}$, MP2 electron-proton correlation energy $E_{e-p}^{C,MP2}$, correlation part of the self-energy of the proton HOMO $\Sigma_{p''}^{C}$. Energies of the HOMO, $\varepsilon_{p''}$, at the KS, G_0W_0, and ev*GW* levels are listed in eV. The scalar-relativistic X2C approach is only applied for L-Ag_3H and $Os(CO)_{10}H_2$, while calculations for all other molecules use the non-relativistic framework. Expt. denotes the experimental finding for the respective proton affinity of the deprotonated species. The same experimental reference values[147–151] as in Ref. [6] were used. For H_2O,[152] HF,[153] and HCl[154] experimental proton binding energies are listed. Quantum protons are marked in bold.

Molecule	H	$E_{e-p}^{C,RPA}$	$E_{e-p}^{C,MP2}$	$\Sigma_{p''}^{C}$	$\varepsilon_{p''}^{KS}$	$\varepsilon_{p''}G_0W_0$	$\varepsilon_{p''}^{evGW}$	Expt.
		[mH]	[mH]	[eV]	[eV]	[eV]	[eV]	[eV]
HCOO**H**	1	−6.88	−9.29	8.76	−23.27	−14.51	−15.36	14.97
CH_3COO**H**	1	−6.84	−9.24	8.87	−23.60	−14.73	−15.54	15.11
CH_3CH_2COO**H**	1	−6.84	−9.25	8.92	−23.63	−14.71	−15.49	15.07
$CH_3CH_2CH_2COO$**H**	1	−6.86	−9.27	8.95	−23.67	−14.71	−15.49	15.03
$CH_3CH_2CH_2CH_2COO$**H**	1	−6.85	−9.25	8.96	−23.66	−14.70	−15.47	15.01
C_6H_5COO**H**	1	−6.89	−9.30	9.10	−23.60	−14.50	−15.04	14.75
CH_2ClCOO**H**	1	−6.64	−8.95	8.92	−23.16	−14.24	−15.00	14.58
$ClCH_2CH_2COO$**H**	1	−6.84	−9.24	8.98	−23.34	−14.36	−15.12	14.78
CH_2FCOO**H**	1	−6.64	−8.95	8.87	−23.16	−14.29	−15.09	14.71
CHF_2COO**H**	1	−6.85	−9.25	8.84	−22.78	−13.94	−14.76	14.32
CF_3COO**H**	1	−6.79	−9.17	8.80	−22.42	−13.62	−14.46	13.99
CH_3COCOO**H**	1	−6.82	−9.20	8.92	−23.10	−14.19	−14.96	14.46
NH_4^+	4	−6.73	−9.07	8.59	−16.79	−8.20	−8.92	8.85
$(CH)NH_2^+$	2	−6.89	−9.31	9.41	−18.37	−8.96	−9.65	9.63
$(CH)NH^+$	1	−6.93	−9.38	9.72	−18.84	−9.12	−9.82	9.84
$CHNH_3^+$	3	−6.83	−9.23	9.04	−17.70	−8.66	−9.34	9.32
$C_6H_5NH_3^+$	3	−6.81	−9.20	9.45	−18.18	−8.73	−9.27	9.15
$CH_3CH_2NH_3^+$	3	−6.72	−9.09	9.19	−17.99	−8.80	−9.45	9.45
$CH_3CH_2CH_2NH_3^+$	3	−6.83	−9.23	9.24	−18.14	−8.90	−9.52	9.51
C_6H_5O**H**	1	−6.94	−9.39	9.24	−24.13	−14.90	−15.46	15.24
CH_3O**H**	1	−7.03	−9.50	8.83	−25.01	−16.18	−16.77	16.55
CH_4	4	−7.02	−9.52	10.08	−28.02	−17.94	−18.65	18.07
HNO_2	1	−6.96	−9.42	9.13	−23.46	−14.32	−15.31	14.75
H_2S	2	−6.61	−8.94	10.85	−25.28	−14.43	−15.19	15.31
HCN	1	−6.76	−9.13	9.48	−23.94	−14.46	−15.39	15.31
HF	1	−6.86	−9.22	7.27	−22.52	−15.25	−15.89	16.06
HCl	1	−6.45	−8.70	9.65	−23.34	−13.69	−14.48	14.42
H_2O	2	−6.99	−9.45	8.61	−24.85	−16.25	−16.89	16.93
He**H**He^+	1	−5.24	−6.40	5.16	−6.92	−2.30	−2.25	
F**H**F^-	1	−5.73	−7.67	7.99	−30.96	−22.97	−23.63	
L-Ag_3**H**	1	−6.50	−8.96	12.99	−28.58	−15.59	−15.86	
$Os(CO)_{10}H_2$	2	−6.81	−8.79	13.38	−26.51	−13.13	−13.86	

large, giving rise to large self-energy corrections. The G_0W_0 variant, being non-iterative, suffers from this enlarged quasiparticle correction, being unable to fully correct the initial KS eigenvalue. Self-consistent ev*GW* is, however, well suited to describe proton affinities as shown in Table 1. All trends in proton affinities are well reproduced. For carboxylates, the proton affinity decreases with the number of halogenides attached. Longer alkane chains also lead to a decrease in proton affinity, in accordance with experimental data. Also, a near constant offset of the proton affinity with respect to the quasiparticle energy can be observed for all carboxylates, being easily correctable. For amides, the reproduction of experimental values is remarkable, and the calculated proton affinities are likely within the error of the experiment. All trends are fully reproduced for this class of compounds. The quasiparticle energies obtained small inorganic molecules clearly exhibit the most pronounced deviation from experimental proton affinities. Notably, especially G_0W_0 deviates by up to 1 eV from the reference values, being unable to take into account the interplay between e-e and e-p correlation. The iterative solution of the self-energies, leading to ev*GW*, improves the situation. Yet, the obtained quasiparticle energies still deviate considerably from the reference values.

Mean unsigned errors (MUE) of the ev*GW* proton affinities outlined in Table 2 are in line with the general accuracy of *GW* methods for ionization energies.[128,156–158] The overall accuracy of *GW* methods is similar to that of the second-order polarization propagator (PP2) method,[70,159] which performs better for carboxylates, and worse for inorganic compounds. G_0W_0 specifically struggles to describe the positively charges amines and inorganic compounds, however outperforms ev*GW* for the important class of carboxylates, at least when geometric changes are not accounted for. For HCOOH, a prototypical carboxylate, the stabilizing reorganization energy is estimated to account for 0.36 eV which hints at the ev*GW* results being rather accurate for carboxylates. Contrary, G_0W_0 underestimates the proton binding energies significantly. While recovering some of the e-p correlation, the perturbative character of the G_0W_0 prevents it from yielding quasiparticle energies as remarkably good as for electrons,[128,156–158] with the size of the self-energy correction approaching 10 eV. The latter value is surprisingly large given the rather small e-p correlations found, but outlines that the e-p correlation energy is changing rapidly with fluctuating proton particle numbers.[160] DFT with added e-p correlation performed significantly better than both ev*GW* and PP2, which can be explained by the DFT + epc17-2 approach also taking into account the changes in geometry upon the loss or addition of a proton – at the prize of two separate optimization cycles.

In contrast, using Born-Oppenheimer DFT yields more significant deviations from the experimental reference values than any other method. The deviations of 0.4–0.8 eV lead to neither of them being commendable to be used for assessing proton affinities.

As a final note, we make the reader aware that the common approach of choosing a suitable KS starting point employed in purely electronic *GW* calculations is not satisfactory in multicomponent DFT targeting protons. Protons themselves have highly localized densities, with HF being nearly exact for the proton-proton part of multicomponent DFT. Mixing DFT and exact exchange to improve protonic KS orbital energies is therefore not yielding the desired result. Instead, if one aims at obtaining proton orbital energies that reflect proton binding energies, suitable electron-proton correlation functionals need to be developed.

4. Conclusions

Correlation energies from the random phase approximation and the correlation part of the *GW* self-energy have been derived for multicomponent quantum mechanical methods and subsequently tested for the well studied electron-proton interactions. It was shown that the self-consistent ev*GW* method is able to yield accurate proton affinities. The computational effort has been minimized using a variant of the resolution-of-the-identity approximation. This way, the time needed to calculate the RPA correlation energy and *GW* self-energies is significantly lower than the time required to solve the multicomponent Kohn–Sham equations. Results exhibit the accuracy generally expected for *GW* and RPA methods, with the presented ansatz possessing the appealing feature of being applicable to fermions other than protons without further adaptions being necessary.

Future outlooks include the derivation of new density functional approximations based on first principles, as well as the description of light-matter interactions beyond the Born-Oppenheimer approximation in scale, with methods targeting these fields being currently developed in one of our laboratories.[161–164] As the *GW* quasiparticle energies are key to the Bethe–Salpeter equation (BSE),[46,63,165–169] the latter can be generalized towards multicomponent systems. For electronic excitations, the *GW*-BSE framework is well accepted as a promising alternative to time-dependent DFT[56,170–185] and we expect a similar performance for other fermions and multicomponent applications. Therefore, the present work also provides a solid foundation for excited-state multicomponent studies beyond DFT.

Supporting Information

Supporting Information with the employed Gaussian basis sets in TURBOMOLE format (basis.txt, auxbasis.txt) and the Cartesian coordinates of the molecular structures (structures.zip) is available.

Acknowledgements

We thank Susi Lehtola for providing us with useful input scripts to generate auxiliary basis sets for the quantum proton. C. H. gratefully acknowledges funding from the Volkswagen Stiftung.

Table 2. Mean unsigned errors (MUE) for proton affinities obtained from bare DFT,[6] DFT + epc17-2,[6] second-order particle propagator method,[70] G_0W_0 @TMHF (this work), and ev*GW* @TMHF (this work). All values in eV.

Class	DFT	epc17-2	PP2	G_0W_0	ev*GW*
Amines	0.72	0.05	0.02	0.60	0.08
Aromatics	0.87	0.10	0.26	0.28	0.27
Inorganics	0.79	0.07	0.34	0.70	0.18
Carboxylates	0.78	0.06	0.12	0.28	0.49
Overall	0.78	0.06	0.14	0.47	0.34

Y.J.F. gratefully acknowledges support via the Walter–Benjamin programme funded by the Deutsche Forschungsgemeinschaft (DFG, German Research Foundation) – 518707327. Open Access funding enabled and organized by Projekt DEAL.

Conflict of Interests

The authors declare no conflict of interest.

Data Availability Statement

The data that support the findings of this study are available in the supplementary material of this article.

Keywords: Quantum Chemistry · Density Functional Calculations · Green's Function Methods · Random Phase Approximation · Relativistic Effects

[1] T. Kreibich, E. K. U. Gross, *Phys. Rev. Lett.* **2001**, *86*, 2984.
[2] A. Chakraborty, M. V. Pak, S. Hammes-Schiffer, *Phys. Rev. Lett.* **2008**, *101*, 153001.
[3] T. Kreibich, R. van Leeuwen, E. K. U. Gross, *Phys. Rev. A* **2008**, *78*, 022501.
[4] R. van Leeuwen, E. Gross, *Multicomponent Density-Functional Theory*, pages 93–106, Springer Berlin Heidelberg, Berlin, Heidelberg, Germany **2006**.
[5] J. Messud, *Phys. Rev. A* **2011**, *84*, 052113.
[6] K. R. Brorsen, Y. Yang, S. Hammes-Schiffer, *J. Phys. Chem. Lett.* **2017**, *8*, 3488.
[7] Q. Yu, S. Hammes-Schiffer, *J. Phys. Chem. Lett.* **2020**, *11*, 10106.
[8] F. Pavošević, T. Culpitt, S. Hammes-Schiffer, *Chem. Rev.* **2020**, *120*, 4222.
[9] S. Hammes-Schiffer, *J. Chem. Phys.* **2021**, *155*, 030901.
[10] T.-C. Li, P.-q. Tong, *Phys. Rev. A* **1986**, *34*, 529.
[11] O. Butriy, H. Ebadi, P. L. de Boeij, R. van Leeuwen, E. K. U. Gross, *Phys. Rev. A* **2007**, *76*, 052514.
[12] Y. Yang, T. Culpitt, S. Hammes-Schiffer, *J. Phys. Chem. Lett.* **2018**, *9*, 1765.
[13] Y. Suzuki, S. Hagiwara, K. Watanabe, *Phys. Rev. Lett.* **2018**, *121*, 133001.
[14] Y. Yang, T. Culpitt, Z. Tao, S. Hammes-Schiffer, *J. Chem. Phys.* **2018**, *149*, 084105.
[15] T. Culpitt, Y. Yang, F. Pavošević, Z. Tao, S. Hammes-Schiffer, *J. Chem. Phys.* **2019**, *150*, 201101.
[16] Z. Tao, S. Roy, P. E. Schneider, F. Pavošević, S. Hammes-Schiffer, *J. Chem. Theory Comput.* **2021**, *17*, 5110.
[17] L. Zhao, Z. Tao, F. Pavošević, A. Wildman, S. Hammes-Schiffer, X. Li, *J. Phys. Chem. Lett.* **2020**, *11*, 4052.
[18] T. Udagawa, T. Tsuneda, M. Tachikawa, *Phys. Rev. A* **2014**, *89*, 052519.
[19] M. V. Pak, A. Chakraborty, S. Hammes-Schiffer, *J. Phys. Chem. A* **2007**, *111*, 4522.
[20] A. Chakraborty, M. V. Pak, S. Hammes-Schiffer, *J. Chem. Phys.* **2009**, *131*, 124115.
[21] A. Sirjoosingh, M. V. Pak, S. Hammes-Schiffer, *J. Chem. Theory Comput.* **2011**, *7*, 2689.
[22] A. Sirjoosingh, M. V. Pak, S. Hammes-Schiffer, *J. Chem. Phys.* **2012**, *136*, 174114.
[23] Y. Yang, K. R. Brorsen, T. Culpitt, M. V. Pak, S. Hammes-Schiffer, *J. Chem. Phys.* **2017**, *147*, 114113.
[24] K. R. Brorsen, P. E. Schneider, S. Hammes-Schiffer, *J. Chem. Phys.* **2018**, *149*, 044110.
[25] Z. Tao, Y. Yang, S. Hammes-Schiffer, *J. Chem. Phys.* **2019**, *151*, 124102.
[26] M. Goli, S. Shahbazian, *J. Chem. Phys.* **2022**, *156*, 044104.
[27] L. Deng, Y. Yuan, F. L. Pratt, W. Zhang, Z. Pan, B. Ye, *Phys. Rev. B* **2023**, *107*, 094433.
[28] D. C. Langreth, J. P. Perdew, *Phys. Rev. B* **1977**, *15*, 2884.
[29] F. Furche, *Phys. Rev. B* **2001**, *64*, 195120.
[30] F. Furche, *J. Chem. Phys.* **2008**, *129*, 114105.
[31] H. Eshuis, J. Yarkony, F. Furche, *J. Chem. Phys.* **2010**, *132*, 234114.
[32] G. E. Scuseria, T. M. Henderson, D. C. Sorensen, *J. Chem. Phys.* **2008**, *129*, 231101.
[33] T. M. Henderson, G. E. Scuseria, *Mol. Phys.* **2010**, *108*, 2511.
[34] J. G. Ángyán, R.-F. Liu, J. Toulouse, G. Jansen, *J. Chem. Theory Comput.* **2011**, *7*, 3116.
[35] W. Klopper, A. M. Teale, S. Coriani, T. B. Pedersen, T. Helgaker, *Chem. Phys. Lett.* **2011**, *510*, 147.
[36] M. Kaltak, J. Klimeš, G. Kresse, *J. Chem. Theory Comput.* **2014**, *10*, 2498.
[37] D. Graf, M. Beuerle, H. F. Schurkus, A. Luenser, G. Savasci, C. Ochsenfeld, *J. Chem. Theory Comput.* **2018**, *14*, 2505.
[38] A. Heßelmann, A. Görling, *Mol. Phys.* **2011**, *109*, 2473.
[39] X. Ren, P. Rinke, C. Joas, M. Scheffler, *J. Mater. Sci.* **2012**, *47*, 7447.
[40] G. P. Chen, V. K. Voora, M. M. Agee, S. G. Balasubramani, F. Furche, *Annu. Rev. Phys. Chem.* **2017**, *68*, 421.
[41] S. Grimme, M. Steinmetz, *Phys. Chem. Chem. Phys.* **2016**, *18*, 20926.
[42] S. Fauser, E. Trushin, C. Neiss, A. Görling, *J. Chem. Phys.* **2021**, *155*, 134111.
[43] E. Trushin, A. Thierbach, A. Görling, *J. Chem. Phys.* **2021**, *154*, 014104.
[44] M. Bokdam, J. Lahnsteiner, B. Ramberger, T. Schäfer, G. Kresse, *Phys. Rev. Lett.* **2017**, *119*, 145501.
[45] L. Hedin, *Phys. Rev.* **1965**, *139*, A796.
[46] X. Leng, F. Jin, M. Wei, Y. Ma, *Wiley Interdiscip. Rev.: Comput. Mol. Sci.* **2016**, *6*, 532.
[47] M. J. van Setten, F. Weigend, F. Evers, *J. Chem. Theory Comput.* **2013**, *9*, 232.
[48] F. Aryasetiawan, R. Sakuma, K. Karlsson, *Phys. Rev. B* **2012**, *85*, 035106.
[49] I. Duchemin, X. Blase, *J. Chem. Theory Comput.* **2020**, *16*, 1742.
[50] M. Kehry, W. Klopper, C. Holzer, *J. Chem. Phys.* **2023**, *159*, 044116.
[51] P. Liu, M. Kaltak, J. Klimeš, G. Kresse, *Phys. Rev. B* **2016**, *94*, 165109.
[52] I. Duchemin, X. Blase, *J. Chem. Theory Comput.* **2021**, *17*, 2383.
[53] M. Govoni, G. Galli, *J. Chem. Theory Comput.* **2015**, *11*, 2680.
[54] V. Vlček, E. Rabani, D. Neuhauser, R. Baer, *J. Chem. Theory Comput.* **2017**, *13*, 4997.
[55] A. Förster, L. Visscher, *J. Chem. Theory Comput.* **2020**, *16*, 7381.
[56] A. Förster, L. Visscher, *J. Chem. Theory Comput.* **2022**, *18*, 6779.
[57] Y. Shigeta, H. Nagao, K. Nishikawa, K. Yamaguchi, *J. Chem. Phys.* **1999**, *111*, 6171.
[58] Y. Shigeta, H. Nagao, K. Nishikawa, K. Yamaguchi, *Int. J. Quantum Chem.* **1999**, *75*, 875.
[59] E. J. Baerends, D. E. Ellis, P. Ros, *Chem. Phys.* **1973**, *2*, 41.
[60] X. Ren, P. Rinke, V. Blum, J. Wieferink, A. Tkatchenko, A. Sanfilippo, K. Reuter, M. Scheffler, *New J. Phys.* **2012**, *14*, 053020.
[61] F. Weigend, M. Häser, *Theor. Chem. Acc.* **1997**, *97*, 331.
[62] C. Hättig, F. Weigend, *J. Chem. Phys.* **2000**, *113*, 5154.
[63] C. Holzer, W. Klopper, *J. Chem. Phys.* **2019**, *150*, 204116.
[64] C. Holzer, *J. Chem. Theory Comput.* **2023**, *19*, 3131.
[65] D. Mejía-Rodríguez, A. de la Lande, *J. Chem. Phys.* **2019**, *150*, 174115.
[66] F. Pavošević, B. J. G. Rousseau, S. Hammes-Schiffer, *J. Phys. Chem. Lett.* **2020**, *11*, 1578.
[67] F. Pavošević, Z. Tao, S. Hammes-Schiffer, *J. Phys. Chem. Lett.* **2021**, *12*, 1631.
[68] L. Hasecke, R. A. Mata, *J. Chem. Theory Comput.* **2023**, *19*, 8223.
[69] J. W. Mintmire, B. I. Dunlap, *Phys. Rev. A* **1982**, *25*, 88.
[70] M. Díaz-Tinoco, J. Romero, J. V. Ortiz, A. Reyes, R. Flores-Moreno, *J. Chem. Phys.* **2013**, *138*, 194108.
[71] A. Oschlies, R. W. Godby, R. J. Needs, *Phys. Rev. B* **1995**, *51*, 1527.
[72] P. Pyykkö, *Chem. Rev.* **2012**, *112*, 371.
[73] P. Pyykkö, *Annu. Rev. Phys. Chem.* **2012**, *63*, 45.
[74] T. Saue, *ChemPhysChem* **2011**, *12*, 3077.
[75] J. Autschbach, *J. Chem. Phys.* **2012**, *136*, 150902.
[76] M. Reiher, A. Wolf., *Relativistic Quantum Chemistry – The Fundamental Theory of Molecular Science*, Wiley-VCH, Weinheim, Germany, 2 edition **2015**.
[77] W. Liu (Editor), *Handbook of Relativistic Quantum Chemistry*, Springer, Berlin, Heidelberg, Germany **2017**.
[78] W. Liu, *J. Chem. Phys.* **2020**, *152*, 180901.
[79] W. Kutzelnigg, W. Liu, *J. Chem. Phys.* **2005**, *123*, 241102.
[80] W. Liu, W. Kutzelnigg, *J. Chem. Phys.* **2007**, *126*, 114107.
[81] W. Liu, D. Peng, *J. Chem. Phys.* **2006**, *125*, 044102.
[82] W. Liu, D. Peng, *J. Chem. Phys.* **2006**, *125*, 149901.
[83] M. Iliaš, T. Saue, *J. Chem. Phys.* **2007**, *126*, 064102.
[84] D. Peng, W. Liu, Y. Xiao, L. Cheng, *J. Chem. Phys.* **2007**, *127*, 104106.
[85] W. Liu, D. Peng, *J. Chem. Phys.* **2009**, *131*, 031104.

[86] K. G. Dyall, *J. Chem. Phys.* **1997**, *106*, 9618.
[87] K. G. Dyall, *J. Chem. Phys.* **1998**, *109*, 4201.
[88] K. G. Dyall, T. Enevoldsen, *J. Chem. Phys.* **1999**, *111*, 10000.
[89] K. G. Dyall, *J. Chem. Phys.* **2001**, *115*, 9136.
[90] D. Cremer, W. Zou, M. Filatov, *Wiley Interdiscip. Rev.: Comput. Mol. Sci.* **2014**, *4*, 436.
[91] D. Peng, N. Middendorf, F. Weigend, M. Reiher, *J. Chem. Phys.* **2013**, *138*, 184105.
[92] M. Douglas, N. M. Kroll, *Ann. Phys. (NY)* **1974**, *82*, 89.
[93] B. A. Hess, *Phys. Rev. A* **1986**, *33*, 3742.
[94] G. Jansen, B. A. Hess, *Phys. Rev. A* **1989**, *39*, 6016.
[95] T. Nakajima, K. Hirao, *Chem. Rev.* **2012**, *112*, 385.
[96] M. Reiher, *Wiley Interdiscip. Rev.: Comput. Mol. Sci.* **2012**, *2*, 139.
[97] M. Barysz, A. J. Sadlej, J. G. Snijders, *Int. J. Quantum Chem.* **1997**, *65*, 225.
[98] M. Barysz, A. J. Sadlej, *J. Mol. Struct.: THEOCHEM* **2001**, *573*, 181.
[99] M. Barysz, A. J. Sadlej, *J. Chem. Phys.* **2002**, *116*, 2696.
[100] D. Kedziera, M. Barysz, *Chem. Phys. Lett.* **2007**, *446*, 176.
[101] D. Peng, M. Reiher, *Theor. Chem. Acc.* **2012**, *131*, 1081.
[102] T. Zhang, J. M. Kasper, X. Li, *Localized relativistic two-component methods for ground and excited state calculations*, volume 16, chapter 2, pages 17–37, Elsevier, Amsterdam, The Netherlands **2020**.
[103] D. Peng, M. Reiher, *J. Chem. Phys.* **2012**, *136*, 244108.
[104] J. Seino, H. Nakai, *J. Chem. Phys.* **2012**, *136*, 244102.
[105] J. Seino, H. Nakai, *J. Chem. Phys.* **2013**, *139*, 034109.
[106] Y. J. Franzke, N. Middendorf, F. Weigend, *J. Chem. Phys.* **2018**, *148*, 104410.
[107] Y. J. Franzke, F. Weigend, *J. Chem. Theory Comput.* **2019**, *15*, 1028.
[108] Y. J. Franzke, F. Mack, F. Weigend, *J. Chem. Theory Comput.* **2021**, *17*, 3974.
[109] Y. J. Franzke, *J. Chem. Theory Comput.* **2023**, *19*, 2010.
[110] Y. J. Franzke, J. M. Yu, *J. Chem. Theory Comput.* **2022**, *18*, 323.
[111] Y. J. Franzke, J. M. Yu, *J. Chem. Theory Comput.* **2022**, *18*, 2246.
[112] S. Gillhuber, Y. J. Franzke, F. Weigend, *J. Phys. Chem. A* **2021**, *125*, 9707.
[113] F. Bruder, Y. J. Franzke, F. Weigend, *J. Phys. Chem. A* **2022**, *126*, 5050.
[114] F. Bruder, Y. J. Franzke, C. Holzer, F. Weigend, *J. Chem. Phys.* **2023**, *159*, 194117.
[115] Y. J. Franzke, C. Holzer, *J. Chem. Phys.* **2023**, *159*, 184102.
[116] Y. J. Franzke, F. Bruder, S. Gillhuber, C. Holzer, F. Weigend, *J. Phys. Chem. A* **2024**, *128*, 670.
[117] M. Kehry, Y. J. Franzke, C. Holzer, W. Klopper, *Mol. Phys.* **2020**, *118*, e1755064.
[118] Y. J. Franzke, C. Holzer, F. Mack, *J. Chem. Theory Comput.* **2022**, *18*, 1030.
[119] C. Holzer, Y. J. Franzke, A. Pausch, *J. Chem. Phys.* **2022**, *157*, 204102.
[120] Y. J. Franzke, C. Holzer, J. H. Andersen, T. Begušić, F. Bruder, S. Coriani, F. Della Sala, E. Fabiano, D. A. Fedotov, S. Fürst, S. Gillhuber, R. Grotjahn, M. Kaupp, M. Kehry, M. Krstić, F. Mack, S. Majumdar, B. D. Nguyen, S. M. Parker, F. Pauly, A. Pausch, E. Perlt, G. S. Phun, A. Rajabi, D. Rappoport, B. Samal, T. Schrader, M. Sharma, E. Tapavicza, R. S. Treß, V. Voora, A. Wodyński, J. M. Yu, B. Zerulla, F. Furche, C. Hättig, M. Sierka, D. P. Tew, F. Weigend, *J. Chem. Theory Comput.* **2023**, *19*, 6859.
[121] S. G. Balasubramani, G. P. Chen, S. Coriani, M. Diedenhofen, M. S. Frank, Y. J. Franzke, F. Furche, R. Grotjahn, M. E. Harding, C. Hättig, A. Hellweg, B. Helmich-Paris, C. Holzer, U. Huniar, M. Kaupp, A. Marefat Khah, S. Karbalaei Khani, T. Müller, F. Mack, B. D. Nguyen, S. M. Parker, E. Perlt, D. Rappoport, K. Reiter, S. Roy, M. Rückert, G. Schmitz, M. Sierka, E. Tapavicza, D. P. Tew, C. van Wüllen, V. K. Voora, F. Weigend, A. Wodyński, J. M. Yu, *J. Chem. Phys.* **2020**, *152*, 184107.
[122] R. Ahlrichs, M. Bär, M. Häser, H. Horn, C. Kölmel, *Chem. Phys. Lett.* **1989**, *162*, 165.
[123] Developers' version of TURBOMOLE V7.8.1 2024, a development of University of Karlsruhe and Forschungszentrum Karlsruhe GmbH, 1989-2007, TURBOMOLE GmbH, since 2007; available from https://www.turbomole.org (retrieved January 29, 2024).
[124] J. Jaramillo, G. E. Scuseria, M. Ernzerhof, *J. Chem. Phys.* **2003**, *118*, 1068.
[125] P. Plessow, F. Weigend, *J. Comput. Chem.* **2012**, *33*, 810.
[126] H. Bahmann, M. Kaupp, *J. Chem. Theory Comput.* **2015**, *11*, 1540.
[127] C. Holzer, *J. Chem. Phys.* **2020**, *153*, 184115.
[128] C. Holzer, Y. J. Franzke, M. Kehry, *J. Chem. Theory Comput.* **2021**, *17*, 2928.
[129] C. Holzer, Y. J. Franzke, *J. Chem. Phys.* **2022**, *157*, 034108.
[130] F. Weigend, R. Ahlrichs, *Phys. Chem. Chem. Phys.* **2005**, *7*, 3297.
[131] I. Samsonova, G. B. Tucker, N. Alaal, K. R. Brorsen, *ACS Omega* **2023**, *8*, 5033.
[132] Q. Yu, F. Pavošević, S. Hammes-Schiffer, *J. Chem. Phys.* **2020**, *152*, 244123.
[133] F. Weigend, *Phys. Chem. Chem. Phys.* **2006**, *8*, 1057.
[134] S. Lehtola, *J. Chem. Theory Comput.* **2021**, *17*, 6886.
[135] S. Lehtola, *J. Chem. Theory Comput.* **2023**, *19*, 6242.
[136] J. Lehtola, M. Hakala, A. Sakko, K. Hämäläinen, *J. Comput. Chem.* **2012**, *33*, 1572.
[137] O. Treutler, *Entwicklung und Anwendung von Dichtefunktionalmethoden*, Dissertation (Dr. rer. nat.), University of Karlsruhe (TH), Germany **1995**.
[138] O. Treutler, R. Ahlrichs, *J. Chem. Phys.* **1995**, *102*, 346.
[139] S. V. Kruppa, C. Groß, X. Gui, F. Bäppler, B. Kwasigroch, Y. Sun, R. Diller, W. Klopper, G. Niedner-Schatteburg, C. Riehn, W. R. Thiel, *Chem. Eur. J.* **2019**, *25*, 11269.
[140] S. A. R. Knox, J. W. Koepke, M. A. Andrews, H. D. Kaesz, *J. Am. Chem. Soc.* **1975**, *97*, 3942.
[141] L. Visscher, K. G. Dyall, *At. Data Nucl. Data* **1997**, *67*, 207.
[142] Y. J. Franzke, L. Spiske, P. Pollak, F. Weigend, *J. Chem. Theory Comput.* **2020**, *16*, 5658.
[143] P. Pollak, F. Weigend, *J. Chem. Theory Comput.* **2017**, *13*, 3696.
[144] Y. J. Franzke, R. Treß, T. M. Pazdera, F. Weigend, *Phys. Chem. Chem. Phys.* **2019**, *21*, 16658.
[145] M. Töpfer, A. Jensen, K. Nagamori, H. Kohguchi, T. Szidarovszky, A. G. Császár, S. Schlemmer, O. Asvany, *Phys. Chem. Chem. Phys.* **2020**, *22*, 22885.
[146] R. Feldmann, A. Baiardi, M. Reiher, *J. Chem. Theory Comput.* **2023**, *19*, 856.
[147] W. Jolly, *Modern Inorganic Chemistry*, McGraw-Hill, New York, United States **1984**.
[148] E. P. L. Hunter, S. G. Lias, *J. Phys. Chem. Ref. Data* **1998**, *27*, 413.
[149] J. B. Cumming, P. Kebarle, *Can. J. Chem.* **1978**, *56*, 1.
[150] K. M. Ervin, J. Ho, W. C. Lineberger, *J. Phys. Chem.* **1988**, *92*, 5405.
[151] S. T. Graul, M. E. Schnute, R. R. Squires, *Int. J. Mass Spectrom. Ion Processes* **1990**, *96*, 181.
[152] J. R. Smith, J. B. Kim, W. C. Lineberger, *Phys. Rev. A* **1997**, *55*, 2036.
[153] Q. J. Hu, J. W. Hepburn, *J. Chem. Phys.* **2006**, *124*, 074311.
[154] Q. J. Hu, T. C. Melville, J. W. Hepburn, *J. Chem. Phys.* **2003**, *119*, 8938.
[155] T. Schrader, J. Khanifaev, E. Perlt, *Chem. Commun.* **2023**, *59*, 13839.
[156] F. Caruso, M. Dauth, M. J. van Setten, P. Rinke, *J. Chem. Theory Comput.* **2016**, *12*, 5076.
[157] F. Bruneval, M. A. L. Marques, *J. Chem. Theory Comput.* **2013**, *9*, 324.
[158] M. J. van Setten, F. Caruso, S. Sharifzadeh, X. Ren, M. Scheffler, F. Liu, J. Lischner, L. Lin, J. R. Deslippe, S. G. Louie, C. Yang, F. Weigend, J. B. Neaton, F. Evers, P. Rinke, *J. Chem. Theory Comput.* **2015**, *11*, 5665.
[159] L. Pedraza-González, J. Romero, J. Alí-Torres, A. Reyes, *Phys. Chem. Chem. Phys.* **2016**, *18*, 27185.
[160] L.-W. Wang, *Phys. Rev. B* **2010**, *82*, 115111.
[161] B. Zerulla, M. Krstić, D. Beutel, C. Holzer, C. Wöll, C. Rockstuhl, I. Fernandez-Corbaton, *Adv. Mater.* **2022**, *34*, 2200350.
[162] B. Zerulla, R. Venkitakrishnan, D. Beutel, M. Krstić, C. Holzer, C. Rockstuhl, I. Fernandez-Corbaton, *Adv. Opt. Mater.* **2023**, *11*, 2201564.
[163] B. Zerulla, D. Beutel, C. Holzer, I. Fernandez-Corbaton, C. Rockstuhl, M. Krstić, *Adv. Mater.* **2023**, page 2311405.
[164] B. Zerulla, C. Li, D. Beutel, S. Oßwald, C. Holzer, J. Bürck, S. Bräse, C. Wöll, I. Fernandez-Corbaton, L. Heinke, C. Rockstuhl, M. Krstić, *Adv. Funct. Mater.* **2023**, page 2301093.
[165] K. Krause, W. Klopper, *J. Comput. Chem.* **2017**, *38*, 383.
[166] C. Holzer, X. Gui, M. E. Harding, G. Kresse, T. Helgaker, W. Klopper, *J. Chem. Phys.* **2018**, *149*, 144106.
[167] X. Blase, I. Duchemin, D. Jacquemin, *Chem. Soc. Rev.* **2018**, *47*, 1022.
[168] C. Liu, J. Kloppenburg, Y. Yao, X. Ren, H. Appel, Y. Kanai, V. Blum, *J. Chem. Phys.* **2020**, *152*, 044105.
[169] X. Blase, I. Duchemin, D. Jacquemin, P.-F. Loos, *J. Chem. Phys. Lett.* **2020**, *11*, 7371.
[170] S. Körbel, P. Boulanger, I. Duchemin, X. Blase, M. A. L. Marques, S. Botti, *J. Chem. Theory Comput.* **2014**, *10*, 3934.
[171] F. Bruneval, S. M. Hamed, J. B. Neaton, *J. Chem. Phys.* **2015**, *142*, 244101.
[172] D. Jacquemin, I. Duchemin, X. Blase, *J. Chem. Theory Comput.* **2015**, *11*, 5340.
[173] D. Jacquemin, I. Duchemin, X. Blase, *J. Chem. Theory Comput.* **2015**, *11*, 3290.
[174] D. Jacquemin, I. Duchemin, A. Blondel, X. Blase, *J. Chem. Theory Comput.* **2016**, *12*, 3969.

[175] D. Jacquemin, I. Duchemin, A. Blondel, X. Blase, *J. Chem. Theory Comput.* **2017**, *13*, 767.
[176] D. Jacquemin, I. Duchemin, X. Blase, *J. Phys. Chem. Lett.* **2017**, *8*, 1524.
[177] C. Azarias, C. Habert, v. Budzák, X. Blase, I. Duchemin, D. Jacquemin, *J. Phys. Chem. A* **2017**, *121*, 6122.
[178] C. Holzer, W. Klopper, *J. Chem. Phys.* **2017**, *147*, 181101.
[179] X. Gui, C. Holzer, W. Klopper, *J. Chem. Theory Comput.* **2018**, *14*, 2127.
[180] C. Holzer, W. Klopper, *J. Chem. Phys.* **2018**, *149*, 101101.
[181] I. Duchemin, C. A. Guido, D. Jacquemin, X. Blase, *Chem. Sci.* **2018**, *9*, 4430.
[182] P.-F. Loos, M. Comin, X. Blase, D. Jacquemin, *J. Chem. Theory Comput.* **2021**, *17*, 3666.
[183] X. Blase, C. Attaccalite, *Appl. Phys. Lett.* **2011**, *99*, 171909.
[184] C. Faber, P. Boulanger, I. Duchemin, C. Attaccalite, X. Blase, *J. Chem. Phys.* **2013**, *139*, 194308.
[185] I. Duchemin, T. Deutsch, X. Blase, *Phys. Rev. Lett.* **2012**, *109*, 167801.

Manuscript received: February 2, 2024
Revised manuscript received: March 7, 2024
Accepted manuscript online: March 8, 2024
Version of record online: ■■, ■■

RESEARCH ARTICLE

Developing robust methods to describe the behavior of fermions embedded into an electronic system is vital to computationally tackle these complicated quantum systems. Introducing various new approaches, including a common auxiliary subspace multicomponent resolution-of-the-identity approach, this work provides powerful techniques to extract correlation energies and fermion binding energies. A concise list of examples is furthermore provided for future reference.

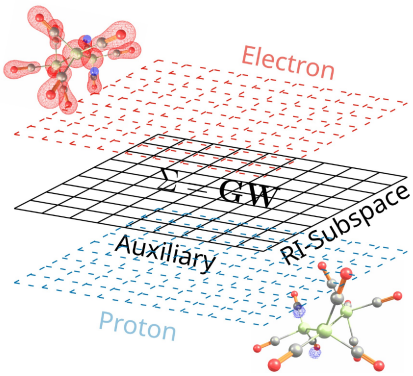

Dr. C. Holzer, Dr. Y. J. Franzke*

1 – 12

Beyond Electrons: Correlation and Self-Energy in Multicomponent Density Functional Theory